

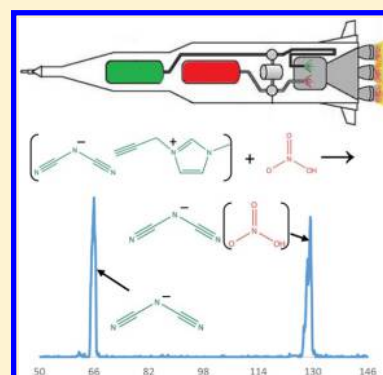
# Experimental and Theoretical Studies of the Reactivity and Thermochemistry of Dicyanamide: $\text{N}(\text{CN})_2^-$

Charles M. Nichols, Zhe-Chen Wang, Zhibo Yang,<sup>†</sup> W. Carl Lineberger, and Veronica M. Bierbaum\*

Department of Chemistry and Biochemistry, JILA, University of Colorado, Boulder, Colorado 80309, United States

## Supporting Information

**ABSTRACT:** Dicyanamide  $[\text{N}(\text{CN})_2^-]$  is a common anionic component of ionic liquids, several of which have shown hypergolic reactivity upon mixing with white-fuming nitric acid. In this study, we explore the thermochemistry of dicyanamide and its reactivity with nitric acid and other molecules to gain insight into the initial stages of the hypergolic phenomenon. We have developed and utilized an electrospray ion source for our selected ion flow tube (SIFT) to generate the dicyanamide anion. We have explored the general reactivity of this ion with several neutral molecules and atoms. Dicyanamide does not show reactivity with  $\text{O}_2$ ,  $\text{H}_2\text{SO}_4$ ,  $\text{H}_2\text{O}_2$ ,  $\text{DBr}$ ,  $\text{HCl}$ ,  $\text{NH}_3$ ,  $\text{N}_2\text{O}$ ,  $\text{SO}_2$ ,  $\text{COS}$ ,  $\text{CO}_2$ ,  $\text{CH}_3\text{OH}$ ,  $\text{H}_2\text{O}$ ,  $\text{CH}_4$ ,  $\text{N}_2$ ,  $\text{CF}_4$ , or  $\text{SF}_6$  ( $k < 1 \times 10^{-12} \text{ cm}^3/\text{s}$ ); moreover, dicyanamide does not react with N atom, O atom, or electronically excited molecular oxygen ( $k < 5 \times 10^{-12} \text{ cm}^3/\text{s}$ ), and our previous studies showed no reactivity with H atom. However, at 0.45 Torr helium, we observe the adduct of dicyanamide with nitric acid with an effective bimolecular rate constant of  $2.7 \times 10^{-10} \text{ cm}^3/\text{s}$ . Intrinsically, dicyanamide is a very stable anion in the gas phase, as illustrated by its lack of reactivity, high electron-binding energy, and low proton affinity. The lack of reactivity of dicyanamide with  $\text{H}_2\text{SO}_4$  gives an upper limit for the gas-phase deprotonation enthalpy of the parent compound ( $\text{HNCNCN}$ ;  $< 310 \pm 3 \text{ kcal/mol}$ ). This limit is in agreement with theoretical calculations at the MP2/6-311++G(d,p) level of theory, finding that  $\Delta H_{298 \text{ K}}(\text{HNCNCN}) = 308.5 \text{ kcal/mol}$ . Dicyanamide has two different proton acceptor sites. Experimental and computational results indicate that it is lower in energy to protonate the terminal nitrile nitrogen than the central nitrogen. Although proton transfer to dicyanamide was not observed for any of the acidic molecules investigated here, the calculations on dicyanamide with one to three nitric acid molecules reveal that higher-order solvation can favor exothermic proton transfer. Furthermore, the formation of 1,5-dinitrobiuret, proposed to be the key intermediate during the hypergolic ignition of dicyanamide ionic liquids with nitric acid, is investigated by calculation of the reaction coordinate. Our results suggest that solvation dynamics of dicyanamide with nitric acid play an important role in hypergolic ignition and the interactions at the droplet/condensed-phase surface between the two hypergolic liquids are very important. Moreover, dicyanamide exists in the atmosphere of Saturn's moon, Titan; the intrinsic stability of dicyanamide strongly suggests that it may exist in molecular clouds of the interstellar medium, especially in regions where other stable carbon–nitrogen anions have been detected.



## INTRODUCTION

Although they have been known for more than 100 years,<sup>1</sup> ionic liquids, or salts with a melting point  $\leq 100 \text{ }^\circ\text{C}$ , have recently received renewed interest in the chemical literature. Ionic liquids exist with a wide variety of cation and anion components; in fact, their properties can be customized by switching or modifying the cations or anions. As a liquid salt, they have many applications. Some synthetic chemists employ ionic liquids as reusable solvents because of their low vapor pressure,<sup>2</sup> and ionic liquids have even been shown to participate in synthesis reactions.<sup>3</sup> Because of their inherent stability, they are being used as the electrolytic medium in batteries, capacitors, and solar cells.<sup>4,5</sup> In addition, a number of materials chemists are investigating ionic liquids as next-generation bipropellant hypergolic fuels in efforts to replace hydrazine based fuels; storage of hydrazine based fuels is challenging because of their toxic, corrosive, and volatile nature. Several ionic liquids exhibit hypergolic behavior,<sup>6–12</sup> providing a possible replacement.

Dicyanamide,  $\text{N}(\text{CN})_2^-$ , is a common anion of ionic liquids; as an anion, it exhibits hypergolic behavior when paired with certain cations. Furthermore, dicyanamide generates ionic liquids with relatively low viscosities, allowing for more efficient delivery in propulsion applications. When paired with 1-propargyl-3-methylimidazolium, the resulting ionic liquid melts at  $17 \text{ }^\circ\text{C}$  and is stable up to  $144 \text{ }^\circ\text{C}$ . Upon mixing with white-fuming nitric acid, 1-propargyl-3-methylimidazolium dicyanamide will undergo hypergolic ignition with a 15 ms delay time.<sup>6</sup> An ignition delay time of  $\leq 5 \text{ ms}$  is preferred for real-world applications; this can be achieved by altering the cation or creating ionic liquid mixtures.<sup>7</sup>

The hypergolic interaction between dicyanamide and nitric acid has been a hot topic of study in the past decade.<sup>6,9,13,14</sup> In 2008, Chambreau and co-workers proposed that 1,5-

Received: December 21, 2015

Revised: February 1, 2016

Published: February 17, 2016

dinitrobiuret is formed during the hypergolic reaction between dicyanamide containing ionic liquids and nitric acid.<sup>9</sup> Since this report, several studies have theoretically investigated the decomposition dynamics of 1,5-dinitrobiuret.<sup>15–17</sup> However, fewer studies have focused on the formation pathway of 1,5-dinitrobiuret. This study will computationally investigate energetics of the previously proposed formation pathway<sup>9</sup> of 1,5-dinitrobiuret through stationary points, including transition states, along the reaction coordinate.

In addition to its unique properties in the liquid phase, dicyanamide is one of the very few anions that has been found not to exhibit reactivity with H atom,<sup>18</sup> the most abundant element in the universe. Dicyanamide is believed to be present in the atmosphere of Saturn's moon Titan.<sup>19</sup> It is also likely a component of the dense interstellar clouds where  $\text{CN}^-$ ,  $\text{C}_3\text{N}^-$ , and  $\text{C}_5\text{N}^-$  have been observed.<sup>20–22</sup> Because of its large electron-binding energy, 4.135 eV,<sup>23</sup> dicyanamide may survive in regions of the interstellar medium where most anions would undergo photodetachment. This study investigates the reactivity of dicyanamide with many astronomically abundant species, including N and O atoms.

## EXPERIMENTAL SECTION

The experiments were carried out at 298 K with a selected ion flow tube (SIFT) that has been modified with a home-built electrospray-ionization (ESI) source. The SIFT has been described in detail previously.<sup>24,25</sup> This work describes the new ESI source, which replaces the source flow tube and electron ionization region; the remaining instrumental details will be covered briefly.

Recently, Viggiano and co-workers reported a new ESI source, designed by Ar dara Corp., for their SIFT.<sup>26</sup> Our ESI design utilizes an ion funnel<sup>27</sup> and is similar to that developed for guided-ion beam experiments.<sup>28,29</sup> A schematic of our ESI source is shown in Figure 1.

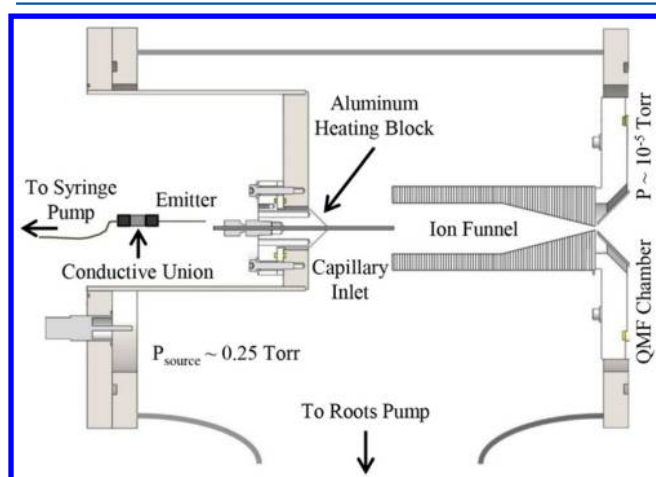


Figure 1. Electrospray ion source for the SIFT.

The ions are generated at ambient pressure by applying a high potential (2–3 kV) to a conductive union. Solution is pushed through this union by a syringe pump with flow rates of 0.2–50  $\mu\text{L}/\text{min}$ . The charged solution then exits through an emitter made from a fused silica capillary, which has an inner diameter of  $\leq 50 \mu\text{m}$ . The ESI emitter is mounted to an X–Y–Z stage (not shown in Figure 1) and positioned in front of a stainless steel capillary inlet that leads into the vacuum

chamber. The capillary inlet is interchangeable. For the experiments reported, a capillary with an inner diameter of 0.76 mm and a length of 98 mm was used. While these exact dimensions are somewhat arbitrary, we found that, for our experiments, a shorter capillary increased the ion-signal intensity. The capillary inlet is seated in an aluminum block that can be heated from 50 to 175  $^\circ\text{C}$  using heater cartridges and a temperature controller. The entrance capillary is typically biased at 100–300 V. As the ions exit the heated capillary inlet, they enter the vacuum chamber ( $\sim 0.25$  Torr), which is pumped by a high-capacity roots blower and then concentrated by an ion funnel.<sup>27</sup> The ion funnel consists of 101 stainless steel electrodes, but does not contain a “jet disruptor”. The first 100 lenses have both radio frequency (RF) and constant (DC) potentials applied to them. The RF potential amplitude is approximately 25 V peak-to-peak and oscillates at a frequency that can be adjusted; for these experiments, frequencies of 1.5–2.8 MHz were used. Adjacent electrodes are supplied with RF potentials of opposite polarities (180 $^\circ$  out-of-phase). The RF potentials radially confine the ions to the center axis of the funnel. Because the lenses are connected through a resistor network, a potential gradient is applied along the ion funnel. Both the entrance and exit DC potentials are adjustable, and the gradient is typically 10–150 V/(10 cm). This potential gradient transmits the ions toward the differentially pumped mass-selection region. The 101st electrostatic lens of the funnel is supplied with an independently adjustable DC potential. All ESI source potentials discussed are referenced to a common ground which is the stainless steel chamber housing. For more information pertaining to the new source, including hardware and electrical schematic, please view the Supporting Information (SI).

To generate the dicyanamide signal, a  $6 \times 10^{-5}$  M solution of sodium dicyanamide ( $\geq 96\%$ ; Fluka) in acetonitrile (99.8%; Sigma-Aldrich) is used with the ESI source. After the dicyanamide ions are transmitted through the new source region, they are sampled into a differentially pumped mass-selection region that contains a quadrupole mass filter. The mass-selected ions of interest are then injected into the reaction flow tube, maintained at 0.45 Torr, where a flow of helium (99.999%; Airgas) entrains the ions. Before entering the flow tube, the helium is passed through a molecular sieve trap immersed in liquid nitrogen. The ions are thermalized to 298 K through multiple collisions with the helium gas, allowing the determination of rate constants at well-defined temperatures and pressures. Temperature variable studies can be carried out as described previously.<sup>25</sup>

The ions are detected downstream by a differentially pumped triple quadrupole system coupled with an electron multiplier. To illustrate the performance of the ESI source, Figure 2a shows a spectrum of 1-butyl-2,3-dimethylimidazolium cation that was generated from a  $2.4 \times 10^{-4}$  M solution of 1-butyl-2,3-dimethylimidazolium tetrafluoroborate in methanol (99.8%, EMD Millipore). This ion was mass-selected, injected into the flow tube, and detected. Figure 2b shows a spectrum of dicyanamide anion that was generated from a  $6 \times 10^{-5}$  M solution of sodium dicyanamide in acetonitrile (99.8%; Sigma-Aldrich). In this case, all negative ions were injected and detected, but the desired dicyanamide anion dominates the mass spectrum.

To determine the rate constant for the clustering reaction of dicyanamide with nitric acid, a known flow rate of nitric acid is introduced at various distances along the reaction flow tube

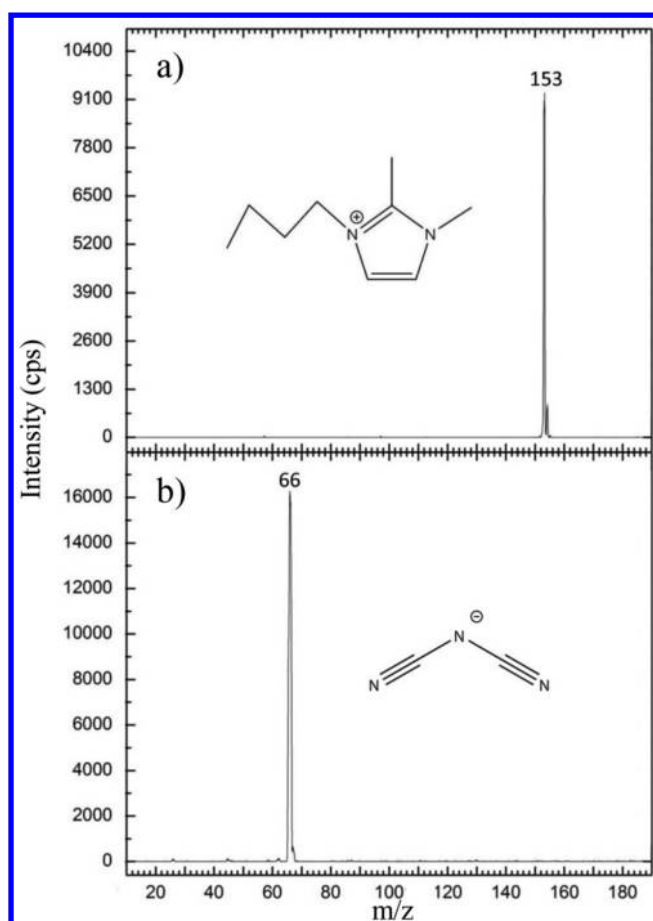


**Figure 2.** ESI generated spectrum of (a) 1-butyl-2,3-dimethylimidazolium and (b) dicyanamide.

through a series of seven inlets. This process depletes the parent dicyanamide anion signal and increases the dicyanamide–nitric acid cluster signal, both of which are monitored with the detection system. Nitric acid is a liquid at room temperature, but it has sufficient vapor pressure for kinetic studies. Since pure nitric acid is not commercially available, we used fuming nitric acid (90%; Alfa Aesar), which contains 10% water. The total nitric acid/water flow was measured by monitoring the pressure change with time in a calibrated volume system. The ratio of vapor pressure of nitric acid to the vapor pressure of water for a 90% solution of nitric acid at 298 K has been previously measured to be 27:1.<sup>30</sup> Using this ratio, we calculated the flow rate of pure nitric acid.

The reactivity of dicyanamide with  $H_2$ ,  $O_2$ ,  $H_2O_2$ ,  $DBr$ ,  $HCl$ ,  $NH_3$ ,  $N_2O$ ,  $SO_2$ ,  $COS$ ,  $CO_2$ ,  $CH_3OH$ ,  $H_2O$ ,  $CH_4$ ,  $N_2$ ,  $CF_4$ , and  $SF_6$  was also investigated, but the reaction rate constants are below the detection limit. The lack of reactivity for these neutral gases was confirmed by introducing a high flow of the neutral gas into the flow tube at the longest reaction distance. Neither dicyanamide depletion nor new ionic products were observed.

We have also investigated the reactivity of dicyanamide with ground state N and O atoms, which were introduced into the reaction flow tube by use of a microwave discharge. Microwave generation of N and O atoms is a well-established technique and has been described by our laboratory previously.<sup>31,32</sup> The N atoms are generated by flowing ( $\sim 0.6 \text{ cm}^3(\text{STP})/\text{s}$ )  $N_2$  gas (99.999%; Airgas) through an Evenson cavity supplied with 50

W of microwave radiation. The overall efficiency of generating N atoms from this technique is approximately 1–3%. The O atoms are then formed by titrating the N atoms with NO (4% in He; Airgas), which forms ground state O atom by the reaction  $N + NO \rightarrow N_2 + O$ . The titration end point for this process is found by plotting the natural log of the ion signal as a function of NO flow. The titration end point reveals the concentration of O atoms introduced into the flow tube and subsequently determines the initial concentration of N atoms in the absence of NO. The microwave discharge is also used to obtain excited state  $O_2$  molecules,  $O_2(^1\Delta)$ . This experiment is performed by flowing  $O_2$  through the microwave discharge. Although no reactivity of dicyanamide anion with  $N(^4S)$ ,  $O(^3P)$ , and  $O_2(^1\Delta)$  was observed, the presence of these neutral reactants was confirmed by studies with other ions that are known to be reactive.

Finally, to investigate the reactivity of dicyanamide with sulfuric acid, we coupled a low-volatility neutral reagent inlet to our reaction flow tube by adapting the methods used by Viggiano et al.<sup>33</sup> A Pyrex bulb was filled with glass wool and then fitted on both ends with 6 mm Pyrex tubing. Approximately 1 mL of sulfuric acid was added to the glass wool. A flow of  $N_2$  ( $\sim 0.2 \text{ cm}^3(\text{STP})/\text{s}$ , UHP; Airgas) enters the glass bulb through a metering valve and flowmeter and carries sulfuric acid into the flow tube. The glass bulb and reagent inlet were heated to approximately 100 °C. Although no reaction was observed between sulfuric acid and dicyanamide, the presence of sulfuric acid was verified by investigating its proton transfer reaction with  $NO_3^-$ , which occurs at the collision rate ( $k \sim 2.6 \times 10^{-9} \text{ cm}^3/\text{s}$ ).<sup>34</sup> Proton transfer was confirmed by observing the loss of  $NO_3^-$  and generation of  $HSO_4^-$ .

## CALCULATIONS

All calculations were carried out with the Gaussian 09 suite of programs.<sup>35</sup> Intermediates and transition states along the potential energy surface for the interaction of dicyanamide with two nitric acid molecules were computed at the B3LYP/aug-cc-pVDZ level of theory. Thermochemical values for dicyanamide and the optimized geometries of dicyanamide clusters with nitric acid are reported using the MP2/6-311++G(d,p) level of theory; MP2/6-311++G(d,p) provides good agreement with experimental results in our previous studies.<sup>36–38</sup> The thermochemical values on the multidimensional reaction coordinate have been corrected for zero-point energy using the rigid-rotor–harmonic-oscillator approximation at 298 K. Transition states were verified by the existence of one imaginary vibrational frequency and confirmed with IRC calculations. Optimized intermediates contain no imaginary frequencies. Cartesian coordinates for the optimized geometries are reported in the SI.

## RESULTS AND DISCUSSION

The dicyanamide anion is a very stable species with an experimental electron-binding energy of  $4.135 \pm 0.010 \text{ eV}$ .<sup>23</sup> Our work studied its reactivity with several neutrals. In efforts to characterize the reactivity of dicyanamide in the gas phase, we explored its reactivity with  $HNO_3$ ,  $H_2SO_4$ ,  $H$ ,  $N$ ,  $O$ ,  $O_2$ ,  $H_2O_2$ ,  $DBr$ ,  $HCl$ ,  $NH_3$ ,  $N_2O$ ,  $SO_2$ ,  $COS$ ,  $CO_2$ ,  $CH_3OH$ ,  $H_2O$ ,  $CH_4$ ,  $N_2$ ,  $CF_4$ , and  $SF_6$ .

However, only one neutral reagent, nitric acid, reacted rapidly enough with dicyanamide for product detection by the SIFT technique. The reaction of dicyanamide with nitric acid

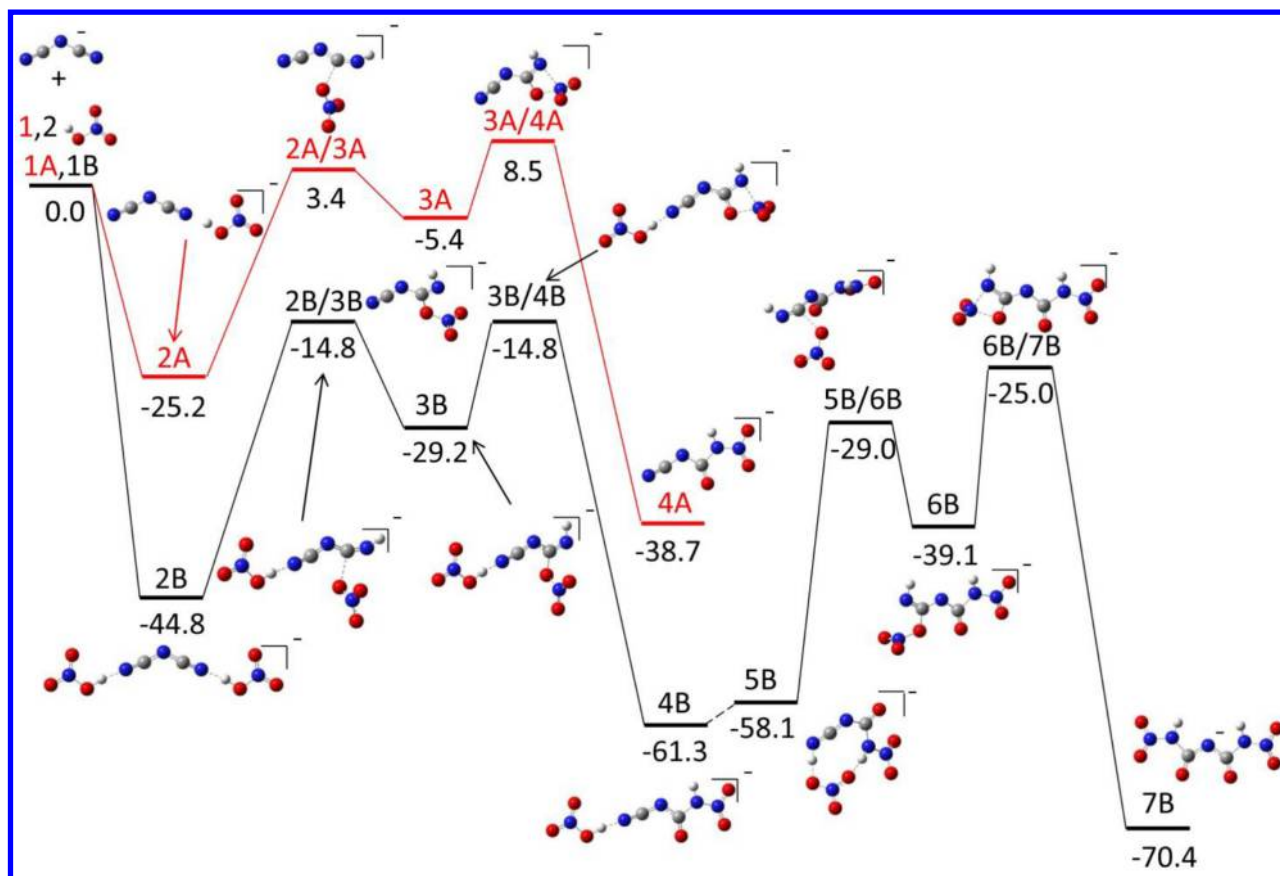


**Figure 3.** Stationary points along the reaction coordinate of dicyanamide with two nitric acid molecules to form deprotonated 1,5-dinitrobiuret. The energies listed are calculated with the B3LYP/Aug-cc-pVDZ method and presented in units of kilocalories per mole. Geometries are posted in the SI.

occurs with an effective bimolecular reaction rate constant of  $2.7 \times 10^{-10} \text{ cm}^3/\text{s}$  at a pressure of 0.45 Torr helium. Only one primary product, the adduct of nitric acid with dicyanamide, was observed. However, subsequent addition of another nitric acid was observed as a secondary product. The full mass spectra for this reaction are provided in the SI.

For the unreactive neutral reagents, we can place an upper limit on their reaction rate constants. These values are estimated based on discernible ion-signal depletion and the number density of the neutral reagent that can be introduced into the reaction flow tube. For the neutral reagents generated from microwave discharge plasmas, i.e., N, O, and  $\text{O}_2(^1\Delta)$ , as well as for sulfuric acid which has low volatility, we designate an upper limit to the reaction rate constant of  $5 \times 10^{-12} \text{ cm}^3/\text{s}$ . For the neutral reagents with high vapor pressures, i.e.,  $\text{O}_2$ ,  $\text{H}_2\text{O}_2$ , DBr, HCl,  $\text{NH}_3$ ,  $\text{N}_2\text{O}$ ,  $\text{SO}_2$ , COS,  $\text{CO}_2$ ,  $\text{CH}_3\text{OH}$ ,  $\text{H}_2\text{O}$ ,  $\text{CH}_4$ ,  $\text{N}_2$ ,  $\text{CF}_4$ , and  $\text{SF}_6$ , we assign an upper limit to their reaction rate constant of  $1 \times 10^{-12} \text{ cm}^3/\text{s}$ . The lack of reactivity with  $\text{O}(^3\text{P})$  and  $\text{O}_2(^1\Delta)$  is surprising, as these reagents are highly reactive with a wide variety of reagents. The absence of reactivity with  $\text{H}_2\text{SO}_4$  allows us to put an upper limit on the deprotonation enthalpy of the parent molecule, HNCNCN, of  $\Delta H < 310 \pm 3 \text{ kcal/mol}$ .

The lack of reactivity of dicyanamide has some important interstellar implications; i.e., dicyanamide could survive the harsh chemical conditions of the interstellar medium (ISM) as it will not react with the abundant atomic species,  $\text{H}(^2\text{S})$ ,  $\text{O}(^3\text{P})$ , and  $\text{N}(^4\text{S})$ . Furthermore, the neutral molecules  $\text{NH}_3$ ,  $\text{H}_2\text{O}$ ,  $\text{CH}_3\text{OH}$ ,  $\text{H}_2$ , COS,  $\text{SO}_2$ ,  $\text{CH}_4$ ,  $\text{N}_2\text{O}$ ,  $\text{N}_2$ , and  $\text{O}_2$  have been detected in the ISM,<sup>39–48</sup> but our experimental results

show no detectable reactivity with dicyanamide. Additionally, a recent rendezvous of Saturn's moon Titan by the Cassini spacecraft provided a negative-ion mass spectrum of Titan's nitrogen- and methane-rich atmosphere. Dicyanamide is inferred to be present, as there is a strong presence of  $m/z$  66 and several other peaks corresponding to adducts of  $m/z$  66 with neutral species, including HCN, HCCH, and  $\text{H}_2$ .<sup>19</sup> The presence of dicyanamide is not surprising, since the components of dicyanamide, i.e., N and C atoms, are abundant in Titan's atmosphere. The intense ionization environment intrinsic to planetary atmospheres could provide a synthesis route for dicyanamide, and upon its formation dicyanamide will be long-lived due to its chemical stability. A laboratory study of the microwave spectrum of dicyanamide—which is a bent molecule with a calculated dipole moment of approximately 1 D—would allow observational astronomers to search for its presence in the interstellar medium.

## ■ FORMATION OF 1,5-DINITROBIURET

The mixing of nitric acid with ionic liquids containing the dicyanamide anion results in hypergolic behavior.<sup>6</sup> For this reason, the fundamental interaction between nitric acid and dicyanamide is of great interest. An insightful study by Chambreau and co-workers acquired infrared spectra of the evolved vapor of 1-butyl-3-methylimidazole dicyanamide with nitric acid.<sup>9</sup> Their work suggests a mechanism where dicyanamide interacts with two nitric acid molecules to form deprotonated 1,5-dinitrobiuret; their studies computationally defined the thermochemical energetics of several reactions. However, they did not characterize the entire mechanism;

therefore, we have calculated stationary points along a multidimensional surface for the gas-phase interaction of dicyanamide with one and two nitric acid molecules (Figure 3).

The multidimensional potential energy diagram of dicyanamide with nitric acid to form 1,5-dinitrobiuret illuminates several interesting points. First, the formation of dicyanamide–nitric acid clusters are highly exothermic by 25 kcal/mol [2A] and 45 kcal/mol [2B] for the addition of one or two nitric acid molecules, respectively. Second, for our experiment, the interaction of dicyanamide with one nitric acid is limited to forming the hydrogen-bonded cluster [2A] because transferring the nitrate to the nitrile carbon [3A] must overcome an endothermic barrier of 3 kcal/mol [2A/3A]. Conversely, the addition of a second nitric acid lowers the transition states below the energy of the reactants, therefore supporting Chambreau's proposed formation of 1,5-dinitrobiuret. Although it is possible that we are generating 1,5-dinitrobiuret as a secondary product in our flow tube, we cannot confirm the structure; in our experiment, products such as [2B], [3B], and [4B], etc., cannot be differentiated because they possess the same mass-to-charge ratio. Finally, the terminal product on the potential energy surface, deprotonated 1,5-dinitrobiuret [7B], is 70 kcal/mol lower in energy than dicyanamide with two nitric acid molecules, suggesting a strong thermodynamic driving force for the formation of 1,5-dinitrobiuret.

#### ■ DICYANAMIDE PROTON AFFINITY AND SOLVENT MOLECULE AFFINITY

An important mechanistic step in the formation of 1,5-dinitrobiuret is proton transfer between nitric acid and dicyanamide. Chambreau's method of forming 1,5-dinitrobiuret requires proton transfer from nitric acid to dicyanamide, followed by subsequent nucleophilic attack on the carbon atom of protonated dicyanamide by nitrate. While our experimental findings provide an upper limit for the proton affinity of dicyanamide ( $<310 \pm 3$  kcal/mol), we have further investigated the proton affinity of dicyanamide computationally with a higher level of theory than was previously reported in the literature, and the lowest-energy structures for the two protonated forms of dicyanamide are shown in Figure 4.

As illustrated, dicyanamide has two protonation sites: the terminal nitrile and central nitrogen. A summary of the calculated and experimentally determined proton affinities of the two protonation sites is provided in Table 1. Our computational studies, as well as computational and experimental reports from the literature, conclude that it is more favorable to protonate dicyanamide on the terminal nitrile nitrogen than on the central nitrogen.<sup>9,49</sup> The B3LYP/6-31+G(d,p) calculations reported by Chambreau et al. and the MP2/6-311++G(d,p) calculations from this work indicate that protonation on the terminal nitrile nitrogen is more favorable than on the central nitrogen by 7.6 and 1.1 kcal/mol, respectively.<sup>9</sup> This discrepancy might arise from differences in the optimized geometry of the centrally protonated tautomer. The optimization of centrally protonated dicyanamide (Figure 4c) at the MP2/6-311++G(d,p) level of theory positions the hydrogen atom out of the molecular plane. This is distinctive between the two levels of theory used, for the same tautomer optimized at the B3LYP level, positioned the hydrogen atom within the molecular plane, thereby preserving the intrinsic  $C_{2v}$  symmetry of dicyanamide. In moving from B3LYP/6-31+G(d,p) to MP2/6-311++G(d,p), the proton affinity of the terminal and central nitrogens of dicyanamide changed by  $-3.1$

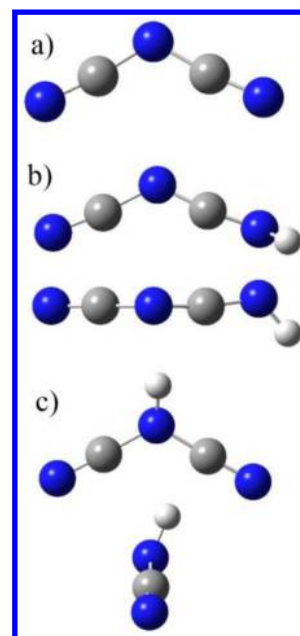


**Figure 4.** Lowest-energy structures of (a) dicyanamide, (b) terminally protonated dicyanamide, and (c) centrally protonated dicyanamide, optimized at the MP2/6-311++G(d,p) level of theory. Geometries posted in the SI.

and 3.4 kcal/mol, respectively, further suggesting that the shift in acidity value for the centrally protonated tautomer occurred in large part due to the differences in the optimized geometry. Nevertheless, even when structures are nearly identical, different theoretical methods can provide different energetic values. Further experimental and computational investigation would be valuable to provide a better understanding of the proton affinity of dicyanamide.

The question remains: is it possible for dicyanamide to accept a proton from nitric acid? In the SIFT experiment, proton transfer is not observed when dicyanamide encounters a single nitric acid molecule at room temperature. Theoretical results support this observation; despite the level of theory employed, proton transfer from nitric acid to dicyanamide is endothermic by at least 15 kcal/mol.

We therefore have conducted calculations to examine higher-order clusters of dicyanamide with nitric acid to explore how proton transfer energetics change as a function of the number of nitric acid molecules in the cluster. Figure 5 shows the optimized geometry of dicyanamide with one, two, and three nitric acid molecules.

When a bimolecular cluster between dicyanamide and one nitric acid forms, the hydrogen-bonded proton resides predominantly on the oxygen atom of nitrate (Figure 5a). However, when an additional nitric acid is added to the cluster, the lowest-energy structure locates the shared proton predominantly on dicyanamide (Figure 5b). Furthermore, adding a third nitric acid molecule onto the final unoccupied nitrate oxygen (Figure 5c) results in a structure where the dicyanamide hydrogen bond length is  $\sim 0.5$  Å shorter than the oxygen–hydrogen bond length.

To further investigate the effects of clustering, the thermochemistry of proton transfer between dicyanamide and nitric acid was investigated for the following reaction.

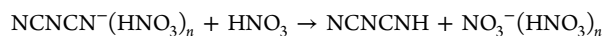
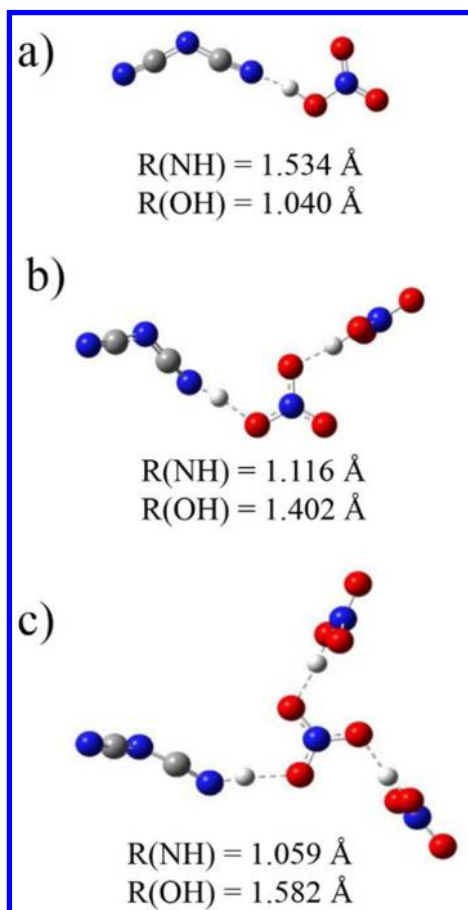


Table 1. Gas-Phase Deprotonation Enthalpy and Acidity of  $\text{HC}_2\text{N}_3$ 

	experiment <sup>a</sup>	theory <sup>a</sup>			
		B3LYP/6-31+G(d,p)	MP2/6-311++G(d,p)		
neutral	$\Delta H_{298\text{K}}$	$\Delta H_{0\text{K}}$	$\Delta H_{0\text{K}}$	$\Delta H_{298\text{K}}$	$\Delta G_{298\text{K}}$
HNCNCN	$<310 \pm 3$	310.4 <sup>b</sup>	307.3	308.5	301.6
HN(CN) <sub>2</sub>	$<310 \pm 3$	302.8 <sup>b</sup>	306.2	307.3	300.8

<sup>a</sup>Units are kilocalories per mole. <sup>b</sup>Previous values; see ref 9.



**Figure 5.** Lowest-energy structures of dicyanamide clustered with one (a), two (b), and three (c) nitric acid molecules optimized at the MP2/6-311++G(d,p) level of theory. Geometries posted in the SI.

The thermodynamic values discussed later are reported for proton transfer to the terminal nitrile nitrogen. For this reaction, when  $n = 0$ , the zero-point thermally corrected enthalpy for reaction at the MP2/6-311++G(d,p) level of theory is 16.6 kcal/mol endothermic. Therefore, in the bimolecular interaction of dicyanamide with nitric acid, proton transfer would not occur. Increasing the solvation of dicyanamide with nitric acid such that  $n = 1$  decreases the endothermicity from 16.6 to 9.8 kcal/mol. Subsequently increasing the solvation to  $n = 2$  and  $n = 3$  further reduces the endothermicity of proton transfer to 4.7 and 3.0 kcal/mol, respectively. This trend and the results from Figure 5 suggest that proton transfer can occur when dicyanamide encounters a cluster of nitric acid molecules such as is possible on the surface of a nitric acid droplet.

The interaction of dicyanamide-containing ionic liquids with nitric acid has been of increasing interest because these liquids hold promise as a next-generation hypergolic fuel. The results

of this study suggest that interactions at the gas–liquid or liquid–liquid interface are very important for hypergolic ignition. These results are consistent with a recent report by Chambreau and co-workers<sup>50</sup> that the basicity ordering of dicyanamide and nitrate is reversed when moving from the gas phase to the condensed phase. Indeed, hypergolic reactivity occurs when a macroscopic droplet of ionic liquid is added to a cuvette containing a macroscopic quantity of nitric acid.<sup>6</sup> For our gas-phase studies, we have determined that solvation of dicyanamide by nitric acid is highly exothermic, and this excess energy can be used to promote energetic chemistry such as, but not limited to, proton transfer; even though the self-sustaining hypergolic reactions are only observed when dicyanamide is paired with certain cations such as 1-propargyl-3-methylimidazolium, “reactivity” is observed even when dicyanamide is paired with inert cations such as  $\text{Na}^+$  or 1-butyl-3-methylimidazolium.<sup>9,13</sup>

## CONCLUSIONS

The dicyanamide anion is extremely stable and exhibits no reactivity with a variety of neutral reagents, including  $\text{H}_2\text{SO}_4$ ,  $\text{H}^2(\text{S})$ ,  $\text{N}^4(\text{S})$ ,  $\text{O}^3(\text{P})$ , and  $\text{O}_2(^1\Delta)$ . Because dicyanamide does not accept a proton from sulfuric acid, an experimental upper limit on the proton affinity is determined as  $<310 \pm 3$  kcal/mol. Conversely, dicyanamide readily clusters with nitric acid, and the ionic adducts are detected in our studies. Our computational results indicate that the association of dicyanamide and nitric acid is exothermic by about 25 kcal/mol. This energy may be responsible for initiating the hypergolic phenomenon that is observed when the two liquids are mixed.

The intrinsic stability of dicyanamide suggests that it may exist in many astrochemical environments; measurement of the microwave spectrum of this anion would allow observational astronomers to search for this species in the interstellar medium.

## ASSOCIATED CONTENT

### Supporting Information

The Supporting Information is available free of charge on the ACS Publications website at DOI: 10.1021/acs.jpca.5b12496.

Additional information relating to the construction and implementation of the electrospray ion (ESI) source, brief discussion about measuring reaction rate constants with the selected ion flow tube, mass spectra for the reaction of dicyanamide with nitric acid, and the geometries of the structures in Figures 3, 4, and 5 (PDF)

## AUTHOR INFORMATION

### Corresponding Author

\*E-mail: [Veronica.Bierbaum@Colorado.EDU](mailto:Veronica.Bierbaum@Colorado.EDU).

## Present Address

<sup>†</sup>Department of Chemistry and Biochemistry, University of Oklahoma, Norman, OK 73019, USA.

## Notes

The authors declare no competing financial interest.

## ACKNOWLEDGMENTS

We gratefully acknowledge support of this work by the Air Force Office of Scientific Research (Grant FA9550-12-1-0125) and the National Science Foundation (Grant CHE-1300886). We are grateful to the Extreme Science and Engineering Discovery Environment (XSEDE), which is supported by the National Science Foundation (Grant ACI-1053575). Any opinion, findings, and conclusions expressed in this material are those of the authors and do not necessarily reflect the views of the National Science Foundation. We appreciate valuable discussions with Dr. Steve Chambreau related to ionic liquids. We also thank Prof. Mary Rodgers and her group for guidance in the design and installation of the ion funnel.

## REFERENCES

- (1) Angell, C. A.; Ansari, Y.; Zhao, Z. F. Ionic Liquids: Past, present and future. *Faraday Discuss.* **2012**, *154*, 9–27.
- (2) Jodry, J. J.; Mikami, K. Ionic Liquids. In *Green reaction media in organic synthesis*, 1st ed.; Mikami, K., Ed.; Blackwell: Kundli, India, 2005; pp 9–54.
- (3) Chiappe, C.; Pieraccini, D. Ionic liquids: solvent properties and organic reactivity. *J. Phys. Org. Chem.* **2005**, *18* (4), 275–297.
- (4) Wishart, J. F. Energy applications of ionic liquids. *Energy Environ. Sci.* **2009**, *2* (9), 956–961.
- (5) Armand, M.; Endres, F.; MacFarlane, D. R.; Ohno, H.; Scrosati, B. Ionic-liquid materials for the electrochemical challenges of the future. *Nat. Mater.* **2009**, *8* (8), 621–629.
- (6) Schneider, S.; Hawkins, T.; Rosander, M.; Vaghjiani, G.; Chambreau, S.; Drake, G. Ionic liquids as hypergolic fuels. *Energy Fuels* **2008**, *22* (4), 2871–2872.
- (7) Li, S. Q.; Gao, H. X.; Shreeve, J. M. Borohydride Ionic Liquids and Borane/Ionic-Liquid Solutions as Hypergolic Fuels with Superior Low Ignition-Delay Times. *Angew. Chem., Int. Ed.* **2014**, *53* (11), 2969–2972.
- (8) Schneider, S.; Hawkins, T.; Ahmed, Y.; Rosander, M.; Hudgens, L.; Mills, J. Green Bipropellants: Hydrogen-Rich Ionic Liquids that Are Hypergolic with Hydrogen Peroxide. *Angew. Chem., Int. Ed.* **2011**, *50* (26), 5886–5888.
- (9) Chambreau, S. D.; Schneider, S.; Rosander, M.; Hawkins, T.; Gallegos, C. J.; Pastewait, M. F.; Vaghjiani, G. L. Fourier transform infrared studies in hypergolic ignition of ionic liquids. *J. Phys. Chem. A* **2008**, *112* (34), 7816–7824.
- (10) McCrary, P. D.; Chatel, G.; Alaniz, S. A.; Cojocar, O. A.; Beasley, P. A.; Flores, L. A.; Kelley, S. P.; Barber, P. S.; Rogers, R. D. Evaluating ionic liquids as hypergolic fuels: Exploring reactivity from molecular structure. *Energy Fuels* **2014**, *28* (5), 3460–3473.
- (11) Zhang, Q. H.; Yin, P.; Zhang, J. H.; Shreeve, J. M. Cyanoborohydride-Based Ionic Liquids as Green Aerospace Bipropellant Fuels. *Chem. - Eur. J.* **2014**, *20* (23), 6909–6914.
- (12) Zhang, Y. Q.; Shreeve, J. M. Dicyanoborate-Based Ionic Liquids as Hypergolic Fluids. *Angew. Chem., Int. Ed.* **2011**, *50* (4), 935–937.
- (13) Litzinger, T.; Iyer, S. Hypergolic Reaction of Dicyanamide-Based Fuels with Nitric Acid. *Energy Fuels* **2011**, *25*, 72–76.
- (14) Catoire, L.; Chambreau, S. D.; Vaghjiani, G. L. Chemical kinetics interpretation of hypergolicity of dicyanamide ionic liquid-based systems. *Combust. Flame* **2012**, *159* (4), 1759–1768.
- (15) Sun, R.; Siebert, M. R.; Xu, L.; Chambreau, S. D.; Vaghjiani, G. L.; Lischka, H.; Liu, J.; Hase, W. L. Direct dynamics simulation of the activation and dissociation of 1,5-dinitrobiuret (HDNB). *J. Phys. Chem. A* **2014**, *118* (12), 2228–2236.
- (16) Russo, M. F.; Bedrov, D.; Singhai, S.; van Duin, A. C. T. Combustion of 1,5-dinitrobiuret (DNB) in the presence of nitric acid using ReaxFF molecular dynamics simulations. *J. Phys. Chem. A* **2013**, *117* (38), 9216–9223.
- (17) Liu, J. B.; Chambreau, S. D.; Vaghjiani, G. L. Thermal decomposition of 1,5-dinitrobiuret (DNB): direct dynamics trajectory simulations and statistical modeling. *J. Phys. Chem. A* **2011**, *115* (28), 8064–8072.
- (18) Yang, Z.; Cole, C. A.; Martinez, O., Jr.; Carpenter, M. Y.; Snow, T. P.; Bierbaum, V. M. Experimental and theoretical studies of reactions between H atoms and nitrogen-containing carbanions. *Astrophys. J.* **2011**, *739* (1), 19.
- (19) Somogyi, A.; Smith, M. A.; Vuitton, V.; Thissen, R.; Komaromi, I. Chemical ionization in the atmosphere? A model study on negatively charged "exotic" ions generated from Titan's tholins by ultrahigh resolution MS and MS/MS. *Int. J. Mass Spectrom.* **2012**, *316*–318, 157–163.
- (20) Thaddeus, P.; Gottlieb, C. A.; Gupta, H.; Brunken, S.; McCarthy, M. C.; Agundez, M.; Guelin, M.; Cernicharo, J. Laboratory and astronomical detection of the negative molecular ion  $C_3N^-$ . *Astrophys. J.* **2008**, *677* (2), 1132–1139.
- (21) Cernicharo, J.; Guelin, M.; Agundez, M.; McCarthy, M. C.; Thaddeus, P. Detection of  $C_3N^-$  and vibrationally excited  $C_6H$  in IRC +10216. *Astrophys. J.* **2008**, *688* (2), L83–L86.
- (22) Agundez, M.; Cernicharo, J.; Guelin, M.; Kahane, C.; Roueff, E.; Klos, J.; Aoi, F. J.; Lique, F.; Marcelino, N.; Goicoechea, J. R.; et al. Astronomical identification of  $CN^-$ , the smallest observed molecular anion. *Astron. Astrophys.* **2010**, *517*, L2.
- (23) Jagoda-Cwiklik, B.; Wang, X. B.; Woo, H. K.; Yang, J.; Wang, G. J.; Zhou, M. F.; Jungwirth, P.; Wang, L. S. Microsolvation of the dicyanamide anion:  $[N(CN)_2^-](H_2O)_n$  ( $n = 0–12$ ). *J. Phys. Chem. A* **2007**, *111* (32), 7719–7725.
- (24) Van Doren, J. M.; Barlow, S. E.; DePuy, C. H.; Bierbaum, V. M. The tandem Flowing Afterglow-SIFT-DRIFT. *Int. J. Mass Spectrom. Ion Processes* **1987**, *81*, 85–100.
- (25) Bierbaum, V. M. Go with the flow: Fifty years of innovation and ion chemistry using the flowing afterglow. *Int. J. Mass Spectrom.* **2015**, *377*, 456–466.
- (26) Melko, J. J.; Ard, S. G.; Shuman, N. S.; Pedder, R. E.; Taormina, C. R.; Viggiano, A. A. Coupling an electrospray source and a solids probe/chemical ionization source to a selected ion flow tube apparatus. *Rev. Sci. Instrum.* **2015**, *86* (8), 084101.
- (27) Kelly, R. T.; Tolmachev, A. V.; Page, J. S.; Tang, K. Q.; Smith, R. D. The ion funnel: Theory, implementations, and applications. *Mass Spectrom. Rev.* **2010**, *29* (2), 294–312.
- (28) Moision, R. M.; Armentrout, P. B. An electrospray ionization source for thermochemical investigation with the guided ion beam mass spectrometer. *J. Am. Soc. Mass Spectrom.* **2007**, *18* (6), 1124–1134.
- (29) Chen, Y.; Rodgers, M. T. Structural and energetic effects in the molecular recognition of protonated peptidomimetic bases by 18-Crown-6. *J. Am. Chem. Soc.* **2012**, *134* (4), 2313–2324.
- (30) Taylor, G. B. Vapor pressure of aqueous solutions of nitric acid. *Ind. Eng. Chem.* **1925**, *17*, 633–635.
- (31) Eichelberger, B.; Snow, T. P.; Barckholtz, C.; Bierbaum, V. M. Reactions of H, N, and O atoms with carbon chain anions of interstellar interest: An experimental study. *Astrophys. J.* **2007**, *667* (2), 1283–1289.
- (32) Wang, Z.-C.; Cole, C. A.; Demarais, N. J.; Snow, T. P.; Bierbaum, V. M. Reactions of azine anions with nitrogen and oxygen atoms: Implications for Titan's upper atmosphere and interstellar chemistry. *J. Am. Chem. Soc.* **2015**, *137* (33), 10700–10709.
- (33) Viggiano, A. A.; Seeley, J. V.; Mundis, P. L.; Williamson, J. S.; Morris, R. A. Rate constants for the reactions of  $XO_3^-(H_2O)_n$  ( $X = C, HC, \text{ and } N$ ) and  $NO_3^-(HNO_3)_n$  with  $H_2SO_4$ : Implications for atmospheric detection of  $H_2SO_4$ . *J. Phys. Chem. A* **1997**, *101* (44), 8275–8278.

(34) Viggiano, A. A.; Perry, R. A.; Albritton, D. L.; Ferguson, E. E.; Fehsenfeld, F. C. Stratospheric negative-ion reaction-rates with  $\text{H}_2\text{SO}_4$ . *J. Geophys. Res.* **1982**, *87* (NC9), 7340–7342.

(35) Frisch, M. J.; Trucks, G. W.; Schlegel, H. B.; Scuseria, G. E.; Robb, M. A.; Cheeseman, J. R.; Scalmani, G.; Barone, V.; Mennucci, B.; Peterson, G. A.; et al. *Gaussian 09*, Revision A.1; Gaussian: Wallingford, CT, USA, 2009.

(36) Thomsen, D. L.; Reece, J. N.; Nichols, C. M.; Hammerum, S.; Bierbaum, V. M. Investigating the alpha-effect in gas-phase  $\text{S}_{\text{N}}2$  reactions of microsolvated anions. *J. Am. Chem. Soc.* **2013**, *135* (41), 15508–15514.

(37) Thomsen, D. L.; Nichols, C. M.; Reece, J. N.; Hammerum, S.; Bierbaum, V. M. The alpha-effect and competing mechanisms: The gas-phase reactions of microsolvated anions with methyl formate. *J. Am. Soc. Mass Spectrom.* **2014**, *25* (2), 159–168.

(38) Thomsen, D. L.; Reece, J. N.; Nichols, C. M.; Hammerum, S.; Bierbaum, V. M. The alpha-effect in gas-phase  $\text{S}_{\text{N}}2$  reactions of microsolvated anions: Methanol as a solvent. *J. Phys. Chem. A* **2014**, *118* (37), 8060–8066.

(39) Cheung, A. C.; Rank, D. M.; Townes, C. H.; Thornton, D. D.; Welch, W. J. Detection of  $\text{NH}_3$  molecules in the interstellar medium by their microwave emission. *Phys. Rev. Lett.* **1968**, *21* (25), 1701–1705.

(40) Cheung, A. C.; Rank, D. M.; Townes, C. H.; Thornton, D. D.; Welch, W. J. Detection of water in interstellar regions by its microwave radiation. *Nature* **1969**, *221* (5181), 626–628.

(41) Ball, J. A.; Gottlieb, C. A.; Lilley, A. E.; Radford, H. E. Detection of methyl alcohol in Sagittarius. *Astrophys. J.* **1970**, *162* (3), L203–L219.

(42) Carruthers, G. R. Rocket observation of interstellar molecular hydrogen. *Astrophys. J.* **1970**, *161* (2), L81–L85.

(43) Jefferts, K. B.; Penzias, A. A.; Wilson, R. W.; Solomon, P. M. Detection of interstellar carbonyl sulfide. *Astrophys. J.* **1971**, *168* (3), L111–L113.

(44) Snyder, L. E.; Hollis, J. M.; Ulich, B. L.; Lovas, F. J.; Johnson, D. R.; Buhl, D. Radio detection of interstellar sulfur-dioxide. *Astrophys. J.* **1975**, *198* (2), L81–L84.

(45) Lacy, J. H.; Carr, J. S.; Evans, N. J.; Baas, F.; Achtermann, J. M.; Arens, J. F. Discovery of interstellar methane - observations of gaseous and solid  $\text{CH}_4$  absorption toward young stars in molecular clouds. *Astrophys. J.* **1991**, *376* (2), 556–560.

(46) Ziurys, L. M.; Apponi, A. J.; Hollis, J. M.; Snyder, L. E. Detection of interstellar  $\text{N}_2\text{O}$  - A new molecule containing an N-O bond. *Astrophys. J.* **1994**, *436* (2), L181–L184.

(47) Knauth, D. C.; Andersson, B. G.; McCandliss, S. R.; Moos, H. W. The interstellar  $\text{N}_2$  abundance towards HD 124314 from far-ultraviolet observations. *Nature* **2004**, *429* (6992), 636–638.

(48) Goldsmith, P. F.; Liseau, R.; Bell, T. A.; Black, J. H.; Chen, J.-H.; Hollenbach, D.; Kaufman, M. J.; Li, D.; Lis, D. C.; Melnick, G.; et al. *Herschel* Measurements of molecular oxygen in Orion. *Astrophys. J.* **2011**, *737* (2), 96.

(49) Lotsch, B. V.; Senker, J.; Schnick, W. Characterization of the thermally induced topochemical solid-state transformation of  $\text{NH}_4[\text{N}(\text{CN})_2]$  into  $\text{NCN}=\text{C}(\text{NH}_2)_2$  by the means of X-ray and neutron diffraction as well as Raman and solid-state NMR spectroscopy. *Inorg. Chem.* **2004**, *43* (3), 895–904.

(50) Chambreau, S. D.; Schenk, A. C.; Sheppard, A. J.; Yandek, G. R.; Vaghjiani, G. L.; Maciejewski, J.; Koh, C. J.; Golan, A.; Leone, S. R. Thermal Decomposition Mechanism of Alkylimidazolium Ionic Liquids with Cyano-Functionalized Anions. *J. Phys. Chem. A* **2014**, *118*, 11119–11132.